

# Chapter 1

## Introduction

### 1.1 Underpotential Deposition: A Successful Misnomer?

The deposition of small amounts of metal atoms<sup>1</sup> on a foreign surface at potentials more positive than those predicted by Nernst equation is nowadays popularly known as underpotential deposition (upd). To denote something that involves positive quantities with the prefix under obviously appears as counterintuitive, so we devote a few lines to explain this contradictory denomination. In the fundamental field of the electrocrystallization of bulk metals, it is widely used the concept of overvoltage  $\eta$ , which is defined as:

$$\eta = E - E_{M_{(\text{bulk})}/M_{(\text{aq})}^{z+}} \quad (1.1)$$

where  $E$  is the actual electrode potential, and  $E_{M_{(\text{bulk})}/M_{(\text{aq})}^{z+}}$  is the Nernst equilibrium potential of the reaction:



where  $M_{(\text{bulk})}$  represents the bulk metallic material, and  $M_{(\text{aq})}^{z+}$  stands for an ion in solution, bearing the charge number  $z$ . Due to different kinetic hindrances, it always happens in the case of bulk materials that metal deposits take place when  $E < E_{M_{(\text{bulk})}/M_{(\text{aq})}^{z+}}$  so that in general the overvoltage results with the condition  $\eta < 0$ . Thus, in the case of bulk deposits the overvoltage results always in *negative* values of  $\eta$ . In the case of underpotential deposition, the reverse condition occurs, because

---

<sup>1</sup> By small amounts, we mean a number of atoms that is related to the number of atoms constituting the surface of a metal substrate. Thus, underpotential deposits usually involve submonolayers, monolayers or at the most bilayers.

metal deposition takes place for  $E > E_{M_{(\text{bulk})}/M_{(\text{aq})}^{z+}}$ , so that  $\eta > 0$ . Then, since the term *overvoltage* was already reserved for metal deposition in the  $\eta < 0$  condition, the only possibility left was to denominate the situation  $\eta > 0$  as *undervoltage*, from there the term *underpotential* deposition, which is usually shortened as upd.

## 1.2 The Magic World of Metal Underpotential Deposition

Within electrochemical surface processes, the deposition of a metal onto a foreign metal surface at underpotential opens the way to a whole universe of possibilities for preparing and designing surfaces with a variety of applications. Among them, we can mention electrocatalysis [1–5], production of compound semiconductors [6, 7], determination of metal traces by stripping voltammetry, achieving mercury-free electroanalytical procedures [8–10], design of biosensors [11–14], surface area measurement of metals [15, 16], of particular importance for metallic nanoporous materials [17, 18], design of nanoparticle shape [19–21] and composition [22, 23], fabrication of nanocables [24], nanotripods [25], microstructures with improved Surface Enhanced Raman Spectroscopy activity [26], evaluation of overpotential deposition kinetics of reactive metals [27], etc. The previous enumeration is by no means mutually exclusive, since for example nanoparticle synthesis is oriented to catalysis, and we emphasize that it is just mentioned some sample reviews or recent work.

Since upd involves the growth of a new phase in a two dimensional system, we will see along the chapters of this book that this phenomenon is by itself of fundamental importance for understanding a number of related processes involved in the formation of new phases with this dimensionality.

We illustrate with the aid of Fig. 1.1 the key advantage of electrochemical deposition of a metal concerning adsorption studies, with respect to the same processes achieved from the gas phase. Let us represent the desorption of an adatom M from a substrate S according to the reaction:



where  $M_{\text{vac}}$  represents a metal atom in vacuum. In Fig. 1.1 we show schematically the (free) energy of an atom bonded to a surface as a function of the distance from it. In the case of metallic substrate/adsorbate systems, the binding energy curve exhibits typically a minimum with values in the range  $-3 \leq E_{\text{ads}}(\text{eV}) \leq -5$  with respect to the vacuum level [28], indicating that the desorption energy  $E_{\text{des}}$  must be of this order of magnitude (but with opposite sign). If we consider the thermal energy at room temperature,  $k_{\text{B}}T = 0.025$  eV, we see that the  $E_{\text{des}}$  amounts are

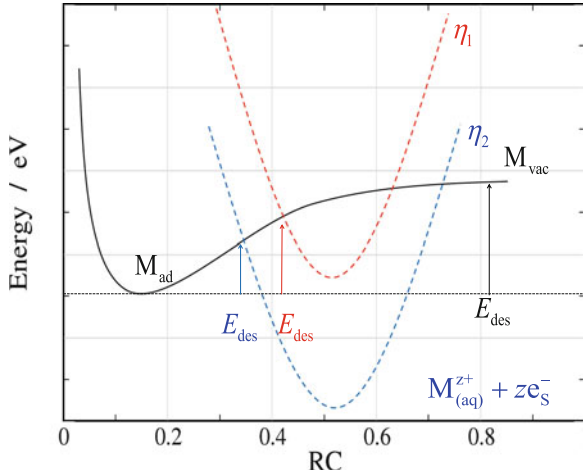


**Fig. 1.1** Schematic comparison between the desorption of a metal adatom from a metal surface by physical detachment (*continuous line*) and electrochemical oxidation (*broken lines*). The *full line* illustrates the free energy curve of the adatom as function of the distance from the surface ( $RC$  reaction coordinate). The *dotted lines* represent the potential energy of the cations in solution plus the electron located in the metal for two different overpotentials, where  $\eta_2 < \eta_1$ . The *arrows* show the point where the potential energy of the adatom and the ion plus electron systems meet. The heights of these arrows give an idea of the activation energy for the detachment process ( $E_{des}$ )

between 120 and 200  $k_B T$ . Taking into account these figures we can make an estimation of the thermal desorption time of an adatom according to:

$$\frac{1}{t_{des}} = \nu \exp[-E_{des}/k_B T] \quad (1.4)$$

where the preexponential factor  $\nu$  contains entropic contributions and shows a weak dependence on the temperature and  $E_{des}$  has been taken as a measure for the activation energy of the desorption process. Inserting into Eq. (1.4) the mentioned limits for  $E_{des}$ , and approximating  $\nu \approx 1 \times 10^{13} \text{ s}^{-1}$ , we get that the desorption times should be in the range  $1 \times 10^{40} < t_{des}(\text{s}) < 7 \times 10^{73}$ . This means that even if we monitor a macroscopic ensemble of adsorbed particles, let us say, of the order of  $\sim 10^{23}$ , we would find desorption times in the interval  $1 \times 10^{17} < t_{des}^{\text{macro}}(\text{s}) < 7 \times 10^{50}$ . To bring into scale the previous curves, we remind that the estimated age of the universe is  $t_{\text{univ}} \approx 4 \times 10^{18} \text{ s}$ . Thus, we arrive to the conclusion that the achievement at room temperature of adsorption/desorption equilibrium is not possible for most S/M metal couples, due to the fact that one of the processes (desorption) is kinetically impossible to achieve. Of course, the previous profiles may be drastically altered by increasing the temperature, but doing this would also promote other processes, like alloying, which are not wished if one is interested on

adsorption studies. What electrochemistry does, as illustrated in the red and the blue lines of Fig. 1.1 is to change reaction (1.3) into:



The dotted curves in Fig. 1.1 introduces an alternative state to that of the desorbed adatom, where now the final state is an ion in solution  $\text{M}_{(\text{aq})}^{+z}$  and an electron (or the number of electrons corresponding to the valence) in the substrate electrode. Since the latter may be polarized, the free energy of electrons in the metal may be changed accordingly, and the desorption barrier may be lowered, as it is indicated by the red and blue arrows in the Fig. 1.1 for two different surface polarizations. It can be seen that the decrease of the barrier for adatom desorption, concomitantly increases the barrier for adsorption. Of course, reality is far more complex than this simple picture and a full theory able to calculate the adsorption and desorption rates accurately for metallic systems is still not available, but the figure illustrates the main idea beyond the electrochemical manipulation of substrate/adsorbate metallic systems, in comparison with a similar process in the gas phase.

From Fig. 1.1 we also visualize that in electrochemistry, the exchange rate between ions in solution and adatoms will be governed by the height of the energy barrier to be surmounted between adatoms and ions, so that it will be determined by the properties of both the metal surface and the solution. This problem has been the subject of extensive consideration in electrochemical textbooks [29] and its nature is starting to be elucidated for specific systems in very recent theoretical work [30].

As stated above, the occurrence of the upd phenomenon results in the formation of a two-dimensional phase, involving in some cases nucleation and growth processes, which take place under the influence of a potential difference [29]. Although the situation is in several aspects similar to the growth of a bulk metallic (three dimensional) phase under electrochemical conditions, there are important differences to take into account.

To go more properly into the peculiarities of upd, let us consider first the problem of the deposition of a bulk metal under equilibrium conditions. This can be described, as it is well known, by a Nernst diagram as the one depicted in Fig. 1.2a. The diagram shows the equilibrium potential  $E_{\text{M}_{(\text{bulk})}/\text{M}_{(\text{aq})}^{z+}}$  for reaction (1.2) as a function of the logarithm of the activity of the cation  $a_{\text{M}_{(\text{aq})}^{z+}}$ , which is given by:

$$E_{\text{M}_{(\text{bulk})}/\text{M}_{(\text{aq})}^{z+}} = E_{\text{M}_{(\text{bulk})}/\text{M}_{(\text{aq})}^{z+}}^0 + \frac{RT}{zF} \ln \left( \frac{a_{\text{M}_{(\text{aq})}^{z+}}}{a_{\text{M}_{(\text{bulk})}}} \right) \quad (1.6)$$

where  $E_{\text{M}_{(\text{bulk})}/\text{M}_{(\text{aq})}^{z+}}^0$  is the standard equilibrium potential,  $a_{\text{M}_{(\text{bulk})}}$  is the activity of the bulk solid (generally assumed to be equal to 1),  $T$  is the temperature,  $R$  and  $F$  correspond to the gas and Faraday constants, respectively. This Figure can be

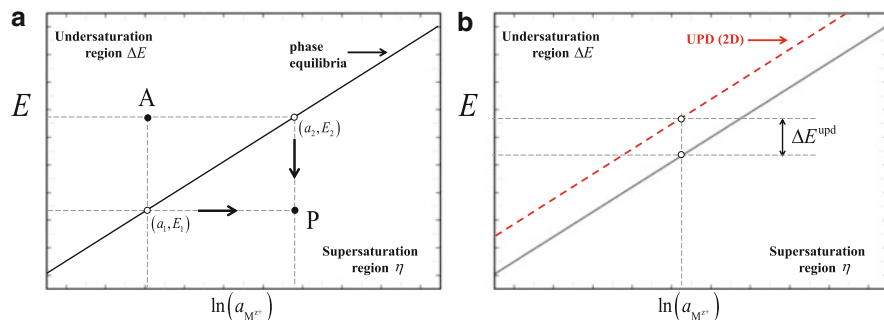


**Fig. 1.2** Qualitative scheme of the variation of the equilibrium dissolution/deposition potential of a metal as a function of ion activity. **(a)** Case of dissolution/deposition of a bulk metal, see Eq. (1.2) in the text. **(b)** Case of underpotential dissolution/deposition of metal M on a foreign substrate S, see Eq. (1.5) in the text. The *continuous black curve* shows the equilibrium conditions for piece of a bulk metal, the *broken red curve* shows the equilibrium line for underpotential deposition conditions. The distance between the two curves is the underpotential shift,  $\Delta E^{\text{upd}}$

envisaged as a phase diagram, where the line denotes coexistence points of the solid phase with the ions in solution and the electrons in the metal. Points above and below the line correspond to situations where, if we force the system to be there, a non-equilibrium state will be reached. For example, if we bring the system to point A, characterized by the pair  $(a_1^A, E_2^A)$ , spontaneous metal dissolution will take place. Alternatively, bringing the system to the conditions of point P, characterized by the pair  $(a_2^P, E_1^P)$ , will result in spontaneous metal deposition. For this reason, we have denoted the previous regions as undersaturation and oversaturation regions respectively.

There are several ways to take the system into these non-equilibrium regions. Let us consider for example the two ways considered in the arrows marked in the Fig. 1.2a, to bring the system to point P, from two different initial equilibrium situations:

1. Increasing  $a_{M^{z+}}^{\text{(aq)}}$  at a constant  $E$  (horizontal arrow).
2. Decreasing  $E$ , at a constant  $a_{M^{z+}}^{\text{(aq)}}$  (vertical arrow).

These processes are marked in Fig. 1.2a as processes  $(a_1, E_1) \rightarrow P$  and  $(a_2, E_2) \rightarrow P$ . Both take to the same point on the oversaturation region, leading to nucleation and growth of the bulk solid phase  $M_{(\text{bulk})}$ . It is interesting to note the dual way that electrochemistry provides to induce nucleation and growth of a new phase. The first path described above has been employed to induce localized electrodeposition using a STM tip [31]. Path 2 is the usual way employed to induce metal growth by a potentiostatic pulse [31, 32].

As mentioned in Eq. (1.1), the magnitude quantifying this displacement from equilibrium is the overpotential  $\eta$ , in such a way that  $\eta < 0$  indicates oversaturation (cathodic overpotentials) and  $\eta > 0$  indicates undersaturation (anodic overpotentials), while  $\eta = 0$  corresponds to phase coexistence.

Although we will see that the proper thermodynamic treatment of upd involves a number of complex features, intuitive knowledge can be gained by proposing in the case of underpotential deposits an heuristic (and rough) extension of Nernst Eq. (1.6) by writing:

$$E_{(M_\theta/S)/M_{(aq)}^{z+}} = E_{M_{(bulk)}/M_{(aq)}^{z+}}^0 + \frac{RT}{zF} \ln \left( \frac{a_{M_{(aq)}^{z+}}}{a_{M_\theta/S}} \right) \quad (1.7)$$

where  $E_{(M_\theta/S)/M_{(aq)}^{z+}}$  denotes the potential at which the  $M_{(aq)}^{z+}$  ions are in equilibrium with the M atoms adsorbed on the surface of S at the coverage  $\theta$ .  $a_{M_\theta/S}$  is the activity of M adsorbed on S at the coverage  $\theta$ . In the limit of multilayer adsorption, Eq. (1.7) reduces to Eq. (1.6), that is,  $a_{M_\theta/S} \rightarrow a_{M_{(bulk)}} = 1$  and  $E_{(M_\theta/S)/M_{(aq)}^{z+}} \rightarrow E_{M_{(bulk)}/M_{(aq)}^{z+}}$ .

In the case of a bulk or surface alloy,  $a_{M_\theta/S}$  decreases with the decreasing fraction of M in the alloy [2, 33]. In the case of monolayers or submonolayers,  $a_{M_\theta/S}$  turns into a function of the surface coverage by adatoms. The presence of a monolayer occurring at underpotentials is equivalent to consider  $a_{M_\theta/S} < 1$ , so that all equilibrium potentials are shifted upwards,  $E_{(M_\theta/S)/M_{(aq)}^{z+}} > E_{M_{(bulk)}/M_{(aq)}^{z+}}$ , see Fig. 1.2b. As a consequence of this shift, the upd curve (red line) falls in the undersaturation region with respect to the bulk equilibrium (black line). That is, the metal M exists on the surface of S at potentials where it should not occur if we think in terms of the bulk M material!

In the case of upd, a magnitude that may be quantified is the so-called underpotential shift, denoted with  $\Delta E^{\text{upd}}$  in Fig. 1.2b. Using Eqs. (1.6) and (1.7) we see that  $\Delta E^{\text{upd}}$  is given by:

$$\Delta E^{\text{upd}} = E_{(M_\theta/S)/M_{(aq)}^{z+}} - E_{M_{(bulk)}/M_{(aq)}^{z+}} \quad (1.8)$$

so that  $\Delta E^{\text{upd}} > 0$  indicates the presence of phases more stable than the prediction of Nernst equation.

As we will see in Chap. 3, the previous argumentation falls too short of being an accurate description, and the curves in Fig. 1.2b do not run parallel. However, we have gained an intuitive introduction to the concept of underpotential shift.

A further complication arises due to the fact that the surface of a real metal electrode is not a perfect arrangement of adsorption sites, but contains a number of imperfections like steps (one-dimensional), kinks and vacancies (zero-dimensional). These defects provide adsorption sites for the formation of deposits that are energetically more favorable than the formation of the monolayer. Thus, if we think in terms of a surface that is progressively polarized towards increasingly negative overpotentials, monolayer growth is preceded by the formation of structures of lower dimensionality [34]. Figure 1.3 shows schematically some of these structures.

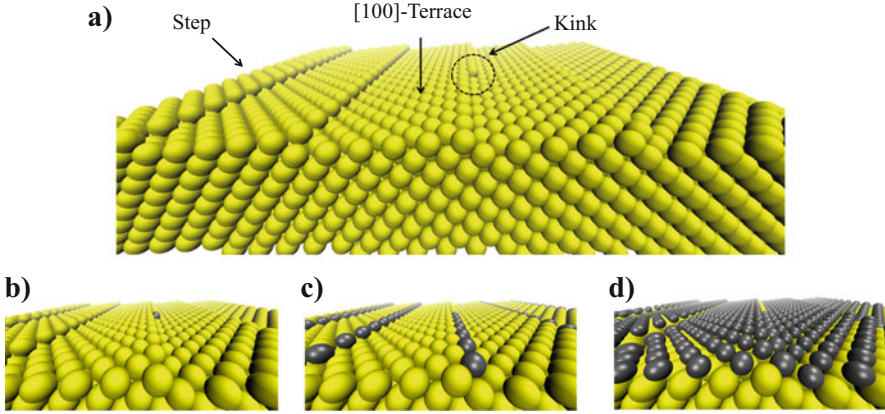


**Fig. 1.3** Stepwise formation of structures of low dimensionality upon application of decreasing overpotentials: (a) defective surface, (b) kink decoration, (c) step decoration, and (d) monolayer formation

To account for the formation of metallic phases with different dimensionalities, an effective Nernst equation may be also proposed:

$$E_{(M_{iD}/S)/M_{(aq)}^{z+}} = E_{M_{(bulk)}/M_{(aq)}^{z+}}^0 + \frac{RT}{zF} \ln \left( \frac{a_{M_{(aq)}^{z+}}}{a_{iD}} \right) \quad \text{with } i = 0, 1 \text{ and } 2 \quad (1.9)$$

where  $E_{(M_{iD}/S)/M_{(aq)}^{z+}}$  is the potential at which the  $M_{(aq)}^{z+}$  ions are in equilibrium with M atom adsorbed on the  $iD$ -structure of S,  $E_{M_{(bulk)}/M_{(aq)}^{z+}}^0$  is the corresponding standard potential and  $a_{iD}$  is an activity, function of structure and dimensionality. The concept of underpotential shift may also be extended according to:

$$\Delta E^{\text{upd}}(iD) = E_{(M_{iD}/S)/M_{(aq)}^{z+}} - E_{M_{(bulk)}/M_{(aq)}^{z+}} \quad \text{with } i = 0, 1 \text{ and } 2 \quad (1.10)$$

Figure 1.4 shows in blue the equilibrium curves corresponding to these low dimensional structures, which follow the ordering:

$$E_{(M_{0D}/S)/M_{(aq)}^{z+}} > E_{(M_{1D}/S)/M_{(aq)}^{z+}} > E_{(M_{2D}/S)/M_{(aq)}^{z+}} > E_{M_{(bulk)}/M_{(aq)}^{z+}} \quad (1.11)$$

where the upd shifts are expected to follow the ordering:

$$\Delta E^{\text{upd}}(0D) > \Delta E^{\text{upd}}(1D) > \Delta E^{\text{upd}}(2D) \quad (1.12)$$

Depending on the magnitude of these differences, several current peaks or their convolution may be present.

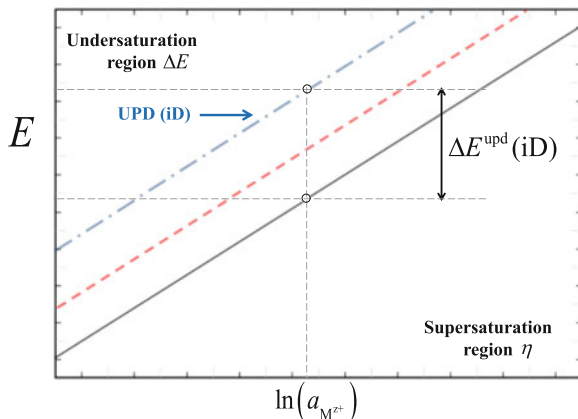


**Fig. 1.4** Qualitative scheme for the variation of the equilibrium dissolution/deposition potential as a function of cation activity. The *continuous black curve* corresponds to equilibrium conditions for a bulk metal surface, the *broken red curve* shows the equilibrium line for 2D underpotential dissolution/deposition and the *blue dotted-broken line* shows the equilibrium condition for underpotential dissolution/deposition of  $i$ -Dimensional structures, with  $i < 2$

The largest contribution to  $\Delta E^{\text{upd}}$  is given by the magnitude of the  $M - S$  binding energy, determined by the following factors [33]:

- (i) the lateral and vertical binding energies between metallic adatoms in nanostructures and the binding energy between adatoms and the substrate,
- (ii) the energetic influence of local surface defects of the substrate,
- (iii) the binding energies between solvent dipoles and the metallic substrate/ nanostructure system, and
- (iv) the binding energies of solvated anions with  $S$  and the metallic nanostructure.

While the first two factors are relatively straightforward to evaluate in terms of models taking into account the metal nature of adsorbate and substrate, the third and fourth elements involve very different interactions (i.e. van der Waals, ionic), which require approximations of considerable complexity.

Concerning effects at the nanoscale, Pliech [35] showed that the equilibrium potential of nanoparticles (NPs),  $E_{M_{(\text{NP})}/M_{(\text{aq})}^{z+}}$ , of a given metal shifts towards more negative potentials with decreasing size. This corresponds to an increase in the free energy of the system and the effect is consistent with an increase in the activity of the metal, that is,  $a_{M_{(\text{NP})}} > 1$ . This behaviour is a consequence of the increasing surface energy of the NP and/or its increasing curvature. The green curve in Fig. 1.5 shows the hypothetical  $E_{M_{(\text{NP})}/M_{(\text{aq})}^{z+}}$  vs  $\ln(a_{M^{z+}})$  curve, exhibiting a negative potential shift, where it is shown that the stability of the pure metal  $M$ -NP occurs in the supersaturation region. In other words, a nanoparticle of a pure metal  $M$  dissolves at potentials where this bulk metal subsists in equilibrium.



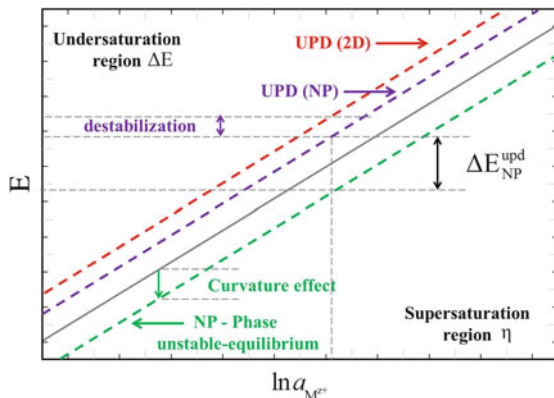


**Fig. 1.5** Qualitative scheme of the variation of the deposition potential as a function of the ion activity for underpotential deposition at the nanoscale. The *continuous black curve* corresponds to equilibrium conditions for a piece of a bulk metal, the *broken red curve* shows the equilibrium line for 2D underpotential deposition, the *green broken line* shows the condition of unstable equilibrium for a metal nanoparticle and the *magenta broken line* show the underpotential deposition on a nanoparticle

However, an underpotential deposit of M on a NP made of a different metal S could in principle show the behaviour depicted by the curve in magenta in Fig. 1.5: it should be less stable than the 2D deposit of M on S (curve in red), but may be more stable than the bulk metal M (curve in black). Thus, the occurrence of upd on NPs will be the result of a delicate balance between substrate/adsorbate interaction and curvature effects, which will be in turn determined by NP size. Chapter 6 is fully dedicated to this type of problems.

### 1.3 Pre-history and Rise of upd

Starting from a very wide viewpoint, we can state that electrochemistry is nowadays a mature science, whose origins dates back to the work of Galvani and Volta, at the end of eighteenth and the beginning of the nineteenth centuries. Its aim is the study of the structure of the interphase between an electric conductor (denominated electrode) and an ionic conductor (denominated electrolyte), or the interphase between two electrolytes [36], and the processes that take place at these interphases. The interphase is the transition region between both phases; its properties differ significantly from those of the corresponding bulk phases. In contrast to this well established knowledge, the recognition of the fact that small quantities of metals may be deposited at potentials more positive than the Nernst reversible potential is relatively more recent. At the beginning, this phenomenon drew particular attention from electrochemists, since at that time the process of nucleation and growth of a

new phase was thought to be a rather simple phenomenon, and not a process involving different stages, as known nowadays.

The first indications for the upd phenomenon were given by Haissinsky in his research on the deposition of radioactive materials [37]. This author [38–40] argued that this phenomenon was due to lattice sites of the substrate presenting large adsorption energies (so called “active centers”). Far from the upd current denomination, at that time the process was addressed as deposition of small metal traces from extremely diluted solutions [41–43]. Shortly after this work, other authors started research on this topic, as for example Rogers [44–52], Kolthoff [53], Haenny [54, 55] and Bowles [56–61]. Current-potential curves (voltammograms) started to be used to analyze traces of Ag deposited on Pt, Cd, Zn and small amounts of Pb on mercury-plated platinum [62–64]. It was soon established that the deposition of these metal traces was very sensitive to the substrate material, and the first attempt to interpret upd through a thermodynamic model was undertaken by Rogers in 1949 [65, 66]. Up to that moment, there was a great controversy concerning the applicability of Nernst equation to describe the deposition potential of these metal traces. The work of Rogers [65] showed the need to consider all the terms in Nernst equation, including the activity of the solid, to describe this phenomenon. Based on the concept drawn by Herzfeld [67] that the activity  $a_{M_0/S}$  of a metal adsorbed on a surface varies proportionally with the fraction of surface covered,  $\theta$ :

$$a_{M_0/S} = f_2 \theta \quad (1.13)$$

where the proportionality constant,  $f_2$ , is denominated activity coefficient of the metal deposit, Rogers [65] proposed a modification to Nernst equation:

$$E = E^0 - E_a - \frac{RT}{zF} \ln \left( \frac{A_e f_1}{V N_a A_a f_2} \left( \frac{C_{ox}}{C - C_{ox}} \right) \right) - \frac{bRT}{zF} \ln (C_g f_g) \quad (1.14)$$

where  $f_1$  is the activity coefficient of the ion,  $C_{ox}$  is the equilibrium concentration of reducible ion,  $C$  is initial molar concentration of reducible (or oxidizable) ions,  $N_a$  is Avogadro’s number,  $A_a$  and  $A_e$  are cross-sectional area, in  $\text{cm}^2$ , of an atom of deposit and area of the electrode in  $\text{cm}^2$ , respectively. The last term in Eq. (1.14) is introduced to consider the activity of a possible complex formed by the ion. The index  $g$  denotes the complex molecule, having  $b$  ligands coordinated with the metal ion being deposited. To consider the changes in the free energy of adsorption, Rogers introduced a new term,  $E_a$  in Eq. (1.14), accounting for the difference between the deposition potential of the metal ion on a surface of similar nature and the deposition potential on a foreign one. Thus, if  $E_a > 0$ , the deposit should be more noble than predicted by Nernst equation. Shortly after the previous contribution, the first indication was found by Mills et al. in 1953 [68] for the dependence of the deposition potential of a given adsorbate on the chemical nature of the substrate electrode. These authors showed that Pb deposition on Au starts at 0.2 V more positive potentials than the deposition potential found on Ag surfaces.

In 1956 Nicholson [69] presented the first computational application to upd, solving numerically [70, 71] the electrochemical problem along with second Fick's law in an IBM 650 computer. This author found a good agreement between the model and experimental data for Ag and Pb deposition on Pt, but found important deviations for Cu deposition on Pt.

Concerning the relationship of upd with early ultra-high vacuum (UHV) experiments on related systems, the articles of Newman [72, 73] and Gruenbaum [74] in UHV showed the presence of a Pb monolayer (and fractions of it) on a Au(111) surface, and evidenced a layer by layer growth up to four monolayers, but the extrapolation to electrochemical systems was not straightforward.

In the 1960s, some authors started to denominate upd as “undervoltage effect” [75], and this phenomenon started to become of wider interest and deserved intensive research [76]. Table 1.1 summarizes work in the area developed in the 1960s decade.

In 1974, Gerischer, Kolb and Przasnyski [94, 95] proposed the first phenomenological theory to explain the origin of upd. Their research on the upd phenomenon showed that the potential difference between upd and bulk deposition could be related to the work function difference between substrate and adsorbate. These authors suggested that the ionic contribution of the bond between the adsorbate and the substrate, given by the partial electron transfer, is the main driving force of the phenomenon. This assumption was supported by the subsequent work of Vijn [96]. Other contributions, like the surface structure of the substrate, the effect of anions

**Table 1.1** Compilation of experimental work undertaken in the 60s concerning upd

Substrate	Adsorbate	References
Pt	Ag	[77]
	Pb	[77, 78]
	Cu	[61, 77, 79–83]
	Ni	[84]
	Au	[84]
	Ce	[78, 85, 86]
	Tl	[56, 57, 61, 86]
	Bi	[61, 78]
	Cd	[61]
	Sn	[61, 60]
Graphite	Hg	[87]
	Ag	[88]
	Cu	[81, 89]
Au	Ni	[84]
	Ag	[75]
	Pb	[90, 91]
Ag	Pb	[76, 92]
	Tl	[76, 93]
Pb	Cd	[76]

and the occurrence of submonolayers or bilayers were not included in this modeling.

At the beginning of the 1970s, attention of experimentalists was focused on the charge status of adsorbates and the effect of the nature of the substrate. Schulze et al. [97–99] and Lorenz et al. [100] reviewed the state-of-the-art of the concept of electroadsorption valency at that time. While this concept will be developed in detail in Chap. 3, we advance that it is related to the flow of charge during the electroadsorption process. At difference with the Nerstian or Faradaic valence, the electroadsorption valency is generally a non-integer number. At the middle of the 1970s different authors showed the importance of performing experiments with well defined metal surfaces, the era of upd on single crystal surfaces was beginning [101–120]. The joint use of electrochemical techniques with Low Energy Electron Diffraction (LEED), Reflected High Energy Electron Diffraction (RHEED), Auger Electron Spectroscopy (AES), Ellipsometry and in situ Specular Reflection Spectroscopy (in situ-SRS) allowed to analyze surface reconstructions, deformations, thicknesses [105, 110, 111, 114, 121–123], different growth types [105, 115], expanded structures like on (100) and (111) surfaces [107, 114], including the occurrence of a second upd monolayer [103].

The study of upd on single crystal surfaces also shed light on nucleation and growth of two-dimensional structures [101, 116, 124–126]. The voltammograms showed better defined and sharper peaks than those obtained with polycrystalline surfaces, and the current-time potentiostatic transients showed possible evidence for the occurrence of first-order phase transitions, or at least the existence of attractive interactions. The possibility of studying these phenomena started to spread over the different research groups. However, the definite answer to some of the questions that arose from these studies is still pending, as we will see along Chaps. 3 and 5. The multiple peaks found in the voltammograms obtained with single crystals rapidly turned into an active subject of research [66–68, 75, 77–93, 126].

The wide research with single crystal surfaces along the 1970s showed that the correlations found by Gerischer, Kolb and Przasnyski [94, 95] could only be applied semiquantitatively to polycrystalline surfaces, since the actual situation concerning single crystal surfaces is considerably more complex [107, 127]. The concept of a binding energy only determined by electronegativity effects was found as insufficient, and the need for more complex models taking into account surface geometry and lateral interactions emerged.

## 1.4 Upd Under the Loupe: Then and Now

In the 1980s the study of upd was favored by the great synergy between the high degree of surface control offered by single crystals and the development of new and powerful surface techniques. The possibility of direct imaging of surfaces and the availability of structural information in direct and reciprocal space gave many answers in the upd field and opened many other ones. Chapters 2 and 3 deal with

these and other studies. The great flexibility of upd to generate surfaces with mixed properties motivated a great body of work using upd systems as model catalytic systems. Chapter 4 deals with application of upd to electrocatalysis.

The massification on computer use, the increasing computer power appearing in the 1990s, as well as the development of new software allowed performing virtual experiments (simulations) of increasing complexity for upd. Chapter 5 reports on these advances.

The advent of nanoscience in the 1990s also reached upd applications in this field, though with a decade of delay. Chapter 6 describes this emerging research area, where upd and galvanic replacement appear as a powerful tool for the design of new materials in the nanoscale.

The new trends and perspectives for upd will be described in Chap. 7.

## References

1. Kokkinidis G (1986) *J Electroanal Chem* 201:217
2. Parsons R, VanderNoot T (1988) *J Electroanal Chem* 257:9
3. Jarvi TD, Stuve EM (1998) In: Lipkowski J, Ross A (eds) *Electrocatalysis*. Wiley-VCH, New York
4. Sánchez CG, Leiva EPM (2003) *Handbook of fuel cell technology*. In: Vielstich W, Lamm A, Gasteiger H (eds) Chapter 5, *Catalysis by upd metals*, vol 2. Wiley, Chichester, pp 47–61
5. Adzic RR (2007) *Electrocatalysis on surfaces modified by metal monolayers deposited at underpotentials*. In: *Encyclopedia of electrochemistry*. Wiley-VCH, Weinheim
6. Gregory BW, Stickney JL (1991) *J Electroanal Chem* 300:543
7. Wade TL, Vaidyanathan R, Happek U, Stickney JL (2001) *J Electroanal Chem* 500:322
8. Beni V, Newton HV, Arrigan DWM, Hill M, Lane WA, Mathewson A (2004) *Anal Chim Acta* 502:195
9. Herzog G, Arrigan DWM (2005) *Trends Anal Chem* 24:208
10. Herzog G, Beni V (2013) *Anal Chim Acta* 769:10
11. Aluoch AO, Sadik OA, Bedi G (2005) *Anal Biochem* 340:136
12. Noah NM, Marcellis O, Almalletti A, Lim J, Sadik OA (2011) *Electroanalysis* 23:2392
13. Li Y, Lu Q, Wu S, Wang L, Shi X (2013) *Biosens Bioelectron* 41:576
14. Ou K-L, Hsue T-C, Liud Y-C, Yang K-H, Tsai H-Y (2014) *Anal Chim Acta* 806:188
15. Chen D, Tao Q, Liao LW, Liu SX, Chen YX, Ye S (2011) *Electrocatal* 2:207
16. Shao M, Odell JH, Choi S-I, Xia Y (2013) *Electrochem Commun* 31:46
17. Liu Y, Bliznakov S, Dimitrov N (2009) *J Phys Chem C* 113:12362
18. Rouya E, Cattarin S, Reed ML, Kelly RG, Zangari G (2012) *J Electrochem Soc* 159:K97
19. Langille MR, Personick ML, Zhang J, Mirkin CA (2012) *J Am Chem Soc* 134:14542
20. Personick ML, Mirkin CA (2013) *J Am Chem Soc* 135:18238
21. Yu Y, Zhang Q, Xie J, Lee JY (2013) *Nat Commun* 4:1454
22. Jiang Y, Jia Y, Zhang J, Zhang L, Huang H, Xie Z, Zheng L (2013) *Chem Eur J* 19:3119
23. Wu Q, Li Y, Xian H, Xu C, Wang L, Chen Z (2013) *Nanotechnology* 24:025501
24. Jie-Ren K et al (2006) U. S. pattern no. 20060024438 A1, Feb 2, 2006
25. Zhang L, Choi S-I, Tao J, Peng H-C, Xie S, Zhu Y, Xie Z, Xia Y (2014) *Adv Funct Mater* 24:7520
26. Plowman BJ, Abdelhamid ME, Ippolito SJ, Bansal V, Bhargava SK, O'Mullane AP (2014) *J Solid State Electrochem* 18:3345

27. Guerra E, Kelsall GH, Bestetti M, Dreisinger D, Wong K, Mitchell KAR, Bizzotto D (2004) *J Electrochem Soc* 151:E1
28. See for example typical cohesive energies of metals in Kittel C (2005) *Introduction to solid state physics*, 8 edn. Wiley, New York
29. Budevski E, Staikov G, Lorenz WJ (1996) *Electrochemical phase formation and growth*. VCH, Weinheim
30. Pinto LMC, Spohr E, Quaino P, Santos E, Schmickler W (2013) *Angew Chem* 125:8037
31. Mariscal MM, Dassie SA (eds) (2007) *Recent advances in nanoscience*. Research Signpost, Trivandrum-Kerala
32. Lipkowski J, Ross PN (1999) *Imaging of surfaces and interfaces*. Wiley-Vch, New York
33. Oviedo OA, Mayer CE, Staikov G, Leiva EPM, Lorenz W (2006) *J Surf Sci* 600:4475
34. Staikov G, Lorenz WJ, Budevski E (1999) In: Ross P, Lipkowski J (eds) *Imaging of surfaces and interfaces – frontiers of electrochemistry*, vol 5. Wiley-VCH, New York, p 1
35. Plieth WJ (1982) *J Phys Chem* 86:3166
36. Schmickler W (1996) *Interfacial electrochemistry*. Oxford University Press, New York
37. Haissinsky M (1933) *Chim Phys* 30:27
38. Haissinsky M (1946) *Electrochimie des Substances Radioactives et des solutions extrêmement diluées*. Actual, Scient No. 1009. Hermann, Paris
39. Haissinsky M (1946) *J Chim Phys* 43:21
40. Haissinsky M (1946) *J Chim Phys* 41:21
41. Haissinsky M, Coche A (1949) *J Chem Soc*:S397
42. Haissinsky M (1952) *Ezperientia* 8:12
43. Danon J, Haissinsky M (1951) *Chim Phys* 48:135
44. Rogers LB, Krause DP, Griess JC Jr, Ehrlinger DB (1949) *J Electrochem Soc* 95(2):33
45. Griess JC Jr, Byrne JT, Rogers LB (1951) *J Electrochem Soc* 98(11):447
46. Rogers IB, Stehney AF (1949) *J Electrochem Soc* 96:25
47. Rogers LB, Miller HH, Goodrich RB, Stehney AF (1949) *Anal Chem* 21:777
48. Byrne JT, Rogers LB (1951) *J Electrochem Soc* 98(11):457
49. Byene JT, Rogers LB, Griess JC Jr (1951) *J Electrochem Soc* 98(11):452
50. Rogers LB (1955) *Rec Chem Prog* 16:197
51. Rogers LB, Merritt C Jr (1953) *J Electrochem Soc* 100(3):131
52. De Geiso RC, Rogers LB (1959) *J Electrochem Soc* 106(5):433
53. Kolthoff IM, Tanaka N (1954) *Anal Chem* 26(4):632
54. Haenny C, Mivalez P (1948) *Helv Chim Acta* 31:633
55. Haenny C, Reymond P (1954) *Helv Chim Acta* 37:2067
56. Bowles BJ (1965) *Electrochim Acta* 10:717
57. Bowles BJ (1965) *Electrochim Acta* 10:731
58. Bowles BJ (1965) *Electrochim Acta* 15:589
59. Bowles BJ (1965) *Electrochim Acta* 15:737
60. Bowles BJ, Cranshaw TE (1965) *Phys Lett* 17:258
61. Bowles BJ (1966) *Nature* 212:1456
62. Lord SS Jr, O'Neill RC, Rogers LB (1952) *Anal Chem* 24:209
63. Gardiner KW, Rogers LB (1953) *ibid* 25:1393
64. Marple TL, Rogers LB (1954) *Anal Chem Acta* 11:574
65. Rogers LB, Stelmey AF (1949) *J Electrochem Soc* 95:25
66. Griess JC, Byrne JT, Rogers LB (1951) *J Electrochem Soc* 98:447
67. Herzfeld KF (1913) *Phys Z* 13:29
68. Mills T, Willis GH (1953) *J Electrochem Soc* 100:452
69. Nicholson MM (1957) *J Am Chem Soc* 79(1):7
70. Rutledge G (1932) *Phys Rev* 40:262
71. Wagner C (1954) *J Math Phys* 32:289
72. Newman RC (1955) Ph.D. Thesis, University of London
73. Newman RC (1957) *Philos Mag* 2:750
74. Gruenbaum E (1958) *Proc Phys Soc Lond* 72:459
75. Probst RC (1968) *J Electroanal Chem* 16:319

76. Astley DJ, Harrison JA, Thirsk HR (1968) *J Electroanal Chem* 19:325
77. Nisbet AR, Bard A (1963) *J Electroanal Chem* 6:332
78. Madi I (1961) *J Inorg Nucl Chem* 22:169
79. Kublik Z (1963) *J Electroanal Chem* 5:450
80. Breiter MW (1967) *J Electrochem Soc* 114:1125
81. Breiter MW (1969) *J Electroanal Chem* 23:173
82. Napp DT, Bruckenstein S (1958) *Anal Chem* 40:1036
83. Tindall GW, Bruckenstein S (1968) *Anal Chem* 40:1051
84. Nicholson MM (1960) *Anal Chem* 32:1058
85. Madi I (1954) *J Inorg Nucl Chem* 26:2149
86. Madi I (1962) *J Inorg Nucl Chem* 24:1501
87. Perone SP, Kretlow J (1965) *Anal Chem* 37:968
88. Perone SP (1963) *Anal Chem* 35:2091
89. Vassos BH, Mark HB Jr (1967) *J Electroanal Chem* 13:1
90. Schmidt E, Gygax HR (1967) *J Electroanal Chem* 13:378
91. Schmidt E, Gygax HR (1967) *J Electroanal Chem* 14:126
92. Schmidt E, Siegenthaler H (1969) *Helv Chim Acta* 52:2245
93. Schmidt E, Wiithrich N (1967) *Helv Chim Acta* 50:2058
94. Kolb DM, Przasnyski M, Gerischer H (1974) *J Electroanal Chem* 54:25
95. Gerischer H, Kolb DM, Przasnyski M (1974) *Surf Sci* 43:662
96. Vijn AK (1974) *Surf Sci* 46:282
97. Vetter KJ, Schultze JW (1972) *Ber Bunsenges Phys Chem* 76:920
98. Vetter KJ, Schultze JW (1972) *Ber Bunsenges Phys Chem* 76:927
99. Schultze JW, Vetter KJ (1973) *J Electroanal Chem* 44:63
100. Lorenz WJ, Salié G (1977) *J Electroanal Chem* 80:1
101. Bewick A, Thomas B (1975) *J Electroanal Chem* 65:911
102. Bewick A, Thomas B (1976) *J Electroanal Chem* 70:239
103. Bewick A, Thomas B (1977) *J Electroanal Chem* 84:127
104. Bewick A, Jovičević JN, Thomas B (1977) *Trans Faraday Disc* 12:24
105. Rawlings KJ, Gibson MJ, Dobson PJ (1978) *J Phys D* 11:2059
106. Dickertmann D, Schultze WJ (1977) *Electrochim Acta* 22:117
107. Schultze JW, Dickertmann D (1976) *Surf Sci* 54:489
108. Dickertmann D, Koppitz FD, Schultze JW (1976) *Electrochim Acta* 21:967
109. Siegenthaler H, Jüttner K (1979) *Electrochim Acta* 24:109
110. Siegenthaler H, Jüttner K, Schmidt E, Lorenz WJ (1978) *Electrochim Acta* 23:1009
111. Jüttner K, Siegenthaler H (1978) *Electrochim Acta* 23:971
112. Staikov G, Jüttner K, Lorenz WJ, Budevski E (1978) *Electrochim Acta* 23:319
113. Staikov G, Jüttner K, Lorenz WJ, Schmidt E (1978) *Electrochim Acta* 23:305
114. Beckmann HO, Gerischer H, Kolb DM, Lehmpfuhl G (1977) *Faraday Symp Chem Soc* 12:51
115. Schultze JW, Dickertmann D (1977) *Faraday Symp Chem Soc* 12:36
116. Bewick A, Jovicevic J, Thomas B (1977) *Faraday Symp Chem Soc* 12:24
117. Herrmann HD, Wiithrich N, Lorenz WJ, Schmidt E (1976) *J Electroanal Chem* 68:289
118. Hilbert F, Mayer C, Lorenz WJ (1973) *J Electroanal Chem* 47:167
119. Jüttner K, Staikov G, Lorenz WJ, Schmidt E (1977) *J Electroanal Chem* 80:67
120. Schultze JW, Dickertmann D (1978) *Ber Bunsenges Phys Chem* 82:528
121. Horkans J, Cahan BD, Yeager E (1975) *J Electrochem Soc* 122:1585
122. Adzic RR, Yeager E, Cahan BD (1974) *J Electrochem Soc* 121:474
123. McIntyre JDE, Kolb DM (1970) *Symp Faraday Soc* 4:99
124. Lorenz WJ, Schmidt E, Staikov G, Bort H (1977) *Faraday Symp Chem Soc* 12:14
125. Bewick A, Thomas B (1977) *J Electroanal Chem* 85:329
126. Lorenz WJ, Herrmann HD, Wuthrich N, Hilbert F (1974) *J Electrochem Soc* 121:1167
127. Bort H, Jüttner K, Lorenz WJ, Schmidt E (1978) *J Electroanal Chem* 90:413